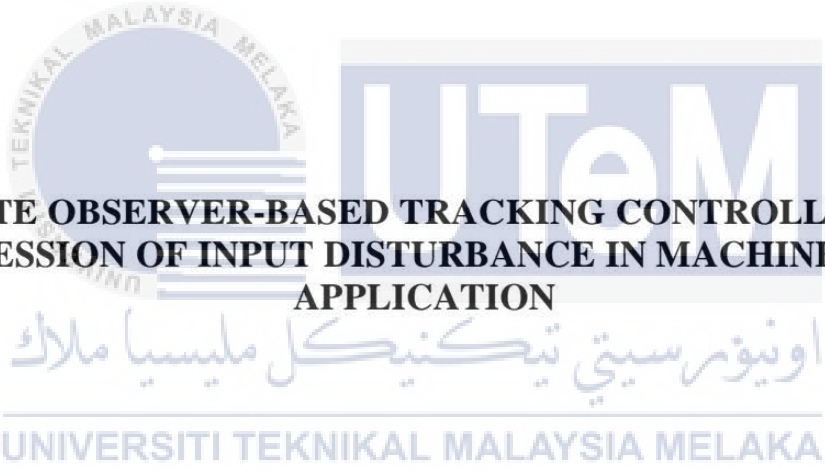




Faculty of Manufacturing Engineering



**A STATE OBSERVER-BASED TRACKING CONTROLLER FOR
SUPPRESSION OF INPUT DISTURBANCE IN MACHINE TOOLS
APPLICATION**

Madihah binti Haji Maharof

Doctor of Philosophy

2021

**A STATE OBSERVER-BASED TRACKING CONTROLLER FOR
SUPPRESSION OF INPUT DISTURBANCE IN MACHINE TOOLS
APPLICATION**

MADIHAH BINTI HAJI MAHAROF



UNIVERSITI TEKNIKAL MALAYSIA MELAKA

2021

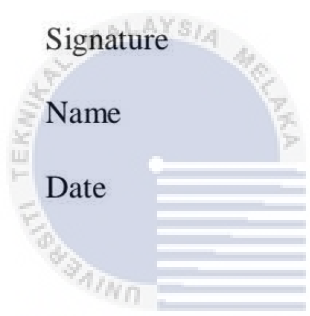
DECLARATION

I declare that this thesis entitled “A State Observer-Based Tracking Controller for Suppression of Input Disturbance in Machine Tools Application” is the result of my own research except as cited in the references. The thesis has not been accepted for any degree and is not concurrently submitted in candidature of any other degree.

Signature : 

Name : Madihah binti Haji Maharof

Date : 1 July 2021



اونيورسيتي تيكنيكل مليسيا ملاك

UNIVERSITI TEKNIKAL MALAYSIA MELAKA

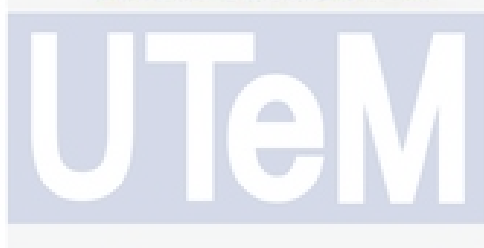
APPROVAL

I hereby declare that I have read this thesis and in my opinion this thesis is sufficient in terms of scope and quality for the award of Doctor of Philosophy in Manufacturing Engineering.

Signature : 

Supervisor Name : Profesor Dr. Zamberi Bin Jamaludin
..... PROFESOR DR. ZAMBERI BIN JAMALUDIN

Date : 1 July 2021 Dekan
Fakulti Kejuruteraan Pembuatan
Universiti Teknikal Malaysia Melaka



اونيورسيتي تيكنيكل مليسيا ملاك

UNIVERSITI TEKNIKAL MALAYSIA MELAKA

DEDICATION

To my beloved mother and mother-in-law,

my husband and my family,

This humble work is dedicated for all of you who taught me to be patience in completing my work, who never fail to give continous support, du'as and encouragement during difficult time of this journey.



ABSTRACT

In milling process, disturbance forces such as cutting force and friction force act directly on the servo drive system producing unwarranted effect that deteriorates the accuracy of the positioning table. This effect has to be compensated in order to preserve geometrical accuracy and quality of the final product. This thesis focuses on suppression of disturbance force characterise by harmonic frequencies dictating by the spindle speed of the milling table using state observer-based controller for precise tracking performances of the motion drive system. This thesis proposes improvement to control performance of classical cascade P/PI controller via add-on modules to the control structure consisting of state observers named inverse model-based disturbance observer (IMBDO) and disturbance force observer (DFO). The cascade P/PI controller was designed using traditional loop shaping frequency domain method. IMBDO estimates the input disturbance and any unmodeled system dynamics while DFO performs direct estimation of the cutting force using information of harmonic frequencies corresponding to the sinusoidal based input disturbance force. Numerical analysis was performed using MATLAB/Simulink software and experimental analysis was performed on the x -axis of an XY milling positioning table ball screw driven system. This thesis compares the performance of cascade P/PI with add-on IMBDO plus DFO with other control configurations; (i) a cascade P/PI stand-alone, (ii) cascade P/PI with IMBDO, and (iii) cascade P/PI with DFO. The control performances of these configurations were analysed using maximum tracking errors (MTE), root mean square (RMSE) of the tracking errors, and magnitudes of the Fast Fourier Transform (FFT) of the tracking errors. Results obtained showed that cascade P/PI with add-on IMBDO plus DFO module produced superior performance against other control configurations. Maximum tracking error results showed that cascade P/PI with IMBDO plus DFO produced the best tracking performances for all harmonic frequencies considered yielding percentage errors reduction of 97.52%, 98.70% and 99.13% for input disturbance of one harmonic, two harmonics, and three harmonics respectively. In term of RMSE values, the experimental results showed that cascade P/PI with IMBDO plus DFO produced the most percentage error reduction with values recorded at 98.80%, 97.75% and 97.97% for the respective input harmonics. In term of FFT results, cascade P/PI with IMBDO plus DFO produced the most reduction in peak amplitudes with values corresponding to 99.78% for the first harmonic, 99.67% and 99.53% for the second harmonics and 99.86%, 99.81% and 99.91% for the third harmonics. The closed loop and sensitivity transfer function of this control configuration confirmed the superiority of cascade P/PI with IMBDO plus DFO in yielding the smallest tracking error thus yielding the most efficient positioning control system.

PENGAWAL PENJEJAKAN BERASASKAN PEMERHATI KEADAAN UNTUK PENINDASAN GANGGUAN INPUT DALAM APLIKASI PERKAKAS MESIN

ABSTRAK

Dalam proses pengisaran, daya gangguan seperti daya pemotongan dan daya geseran yang bertindak secara langsung terhadap permukaan kerja menghasilkan impak luaran kepada sistem pemacu meja kedudukan. Kesan ini mesti dikurangkan untuk memelihara ketepatan geometri dan kualiti produk. Tesis ini memberi tumpuan kepada penekanan daya gangguan, diklasifikasikan oleh frekuensi harmonik yang ditentukan oleh kelajuan gelendong meja pengisaran menggunakan pengawal berdasarkan anggaran untuk pengesanan prestasi yang tepat dalam sistem pemacu gerakan. Tesis ini mencadangkan penambahbaikan bagi mengawal prestasi kawalan dengan menggunakan penganggar yang dinamakan pemerhati gangguan berdasarkan model terbalik (IMBDO) dan daya gangguan pemerhati (DFO) sebagai modul tambahan kepada pengawal konvensional lata P/PI. Pengawal konvensional lata P/PI telah direka menggunakan kaedah domain frekuensi membentuk gelung tradisional. IMBDO menganggarkan gangguan input dan dinamik sistem yang tidak dimodifikasi manakala, DFO melakukan anggaran terus dari daya pemotongan menggunakan maklumat dari frekuensi harmonik yang sesuai dengan daya gangguan berasaskan masukkan sinusoidal. Analisis berangka dilaksanakan dengan menggunakan perisian MATLAB/Simulink dan analisis eksperimen dilaksanakan pada paksi-x sistem pemacu skru bola pemutar XY. Tesis ini membandingkan prestasi pengawal lata P/PI berserta tambahan IMBDO tambah DFO dengan konfigurasi pengawal yang lain iaitu; (i) pengawal lata P/PI, (ii) pengawal lata P/PI dengan IMBDO, dan (iii) pengawal lata P/PI dengan DFO. Prestasi kawalan konfigurasi ini dianalisis menggunakan ralat trajektori maksimum (MTE), ralat purata punca kuasa dua (RMSE) dan magnitud transformasi fourier pantas (FFT). Hasil yang diperolehi menunjukkan pengawal lata P/PI berserta tambahan IMBDO tambah DFO menghasilkan prestasi unggul berbanding konfigurasi pengawal lain. Keputusan MTE menunjukkan pengawal lata P/PI dengan IMBDO tambah DFO menghasilkan prestasi penjejakan terbaik, memandangkan gangguan input satu, dua, dan tiga harmonik masing-masing menghasilkan penurunan peratusan ralat sebanyak 97.52%, 98.70% dan 99.13%. Dari segi nilai RMSE, hasil eksperimen menunjukkan pengawal lata P/PI dengan IMBDO tambah DFO menghasilkan pengurangan ralat peratusan terbanyak masing-masing dengan nilai direkodkan pada 98.80%, 97.75% dan 97.97% input harmonik. Dari segi keputusan FFT menunjukkan pengawal lata P/PI dengan IMBDO tambah DFO menghasilkan penurunan amplitud puncak dengan nilai 99.78% untuk harmonik pertama, 99.67% dan 99.53% untuk harmonik kedua dan 99.86%, 99.81% dan 99.91% untuk harmonik ketiga. Fungsi gelung tertutup dan sensitiviti kawalan bagi konfigurasi pengawal ini mengesahkan keunggulan pengawal lata P/PI dengan IMBDO tambah DFO dalam menghasilkan ralat penjejakan terkecil dan secara tidak langsung menghasilkan sistem kawalan kedudukan yang paling efisien.

ACKNOWLEDGEMENTS

In the Name of Allah, the Most Gracious, the Most Merciful

First and foremost, I would like to thank and praise Allah the Almighty, my Creator, my Sustainer, for everything I received since the beginning of my life. I would like to express my sincere gratitude to my respected supervisor, Professor Dr. Zamberi bin Jamaludin for the continuous support of my study and research, for his patience, motivation, enthusiasm, and immense knowledge. His guidance helped me in all the time of research and writing of this thesis. I would also like to thank my co-supervisor, Associate Professor Ir. Dr. Mohamad bin Minhat for his time, encouragement and effort for sharing knowledge with me.

I would also like to take this opportunity to thank to the Centre for Graduate Studies (PPS), Faculty of Manufacturing Engineering (FKP) and Universiti Teknikal Malaysia Melaka (UTeM) for the facilities provided. Special thanks to Fundamental Research Grant Scheme and MyPhD scholarship by Ministry of Higher Education Malaysia for financial support throughout this research. These financial supports are greatly appreciated and indebted.

I would like to extend my deepest gratitude to my fellow labmates from Control System in Machine Tools (CosMaT) research group, Ir. Dr. Lokman bin Abdullah, Dr. Nur Aidawaty binti Rafan, Dr. Chiew Tsung Heng, Mrs. Nur Amira binti Anang, Mr. Muhammad Azri bin Othman, Mr. Jailani bin Jamaludin, Miss Hidayah binti Seman, Mr. Agus Sudioanto, and Iqbal Afiq bin Saidin for always gives comment, opinion and ideas towards my research and also for their valuable helps in MATLAB. I would like to thank Dr. Maziaty Akmal binti Mohd Hatta, Miss. W. Noor Fatimah binti W. Mohamad, Mrs. Suraya binti Laily, Mrs. Nurhernida binti Abdullah Sani, Dr. Norazlina binti Yatim, and Mr. Mohd Remy bin Ab Karim for always supporting and keeping me motivated throughout this research.

A special thanks also to my mother, my mother-in-law and my family for their prayers, loves, cares and support. I am greatly indebted to them and may Allah repay all their good deeds and sacrifices. Finally and most importantly, a special thanks to a very special person, my husband, Muhamad Faiz Farhan bin Mohamad Shah for his continued and unfailing love, support and understanding during my study.

TABLE OF CONTENTS

| | PAGE |
|---|--------------|
| DECLARATION | |
| APPROVAL | |
| DEDICATION | |
| ABSTRACT | i |
| ABSTRAK | ii |
| ACKNOWLEDGEMENTS | iii |
| TABLE OF CONTENTS | iv |
| LIST OF TABLES | viii |
| LIST OF FIGURES | xiii |
| LIST OF APPENDICES | xxiii |
| LIST OF SYMBOLS | xxiv |
| LIST OF ABBREVIATIONS | xxvii |
| LIST OF PUBLICATIONS | xxix |
| CHAPTER | |
| 1. INTRODUCTION | 1 |
| 1.1 Background | 1 |
| 1.2 Problem statement | 3 |
| 1.3 Research objectives | 5 |
| 1.4 Research scopes and limitations | 5 |
| 1.5 Significant of study | 6 |
| 1.6 Overview of thesis | 7 |
| 1.7 Summary | 8 |
| 2. LITERATURE REVIEW | 9 |
| 2.1 Introduction | 9 |
| 2.2 Mechanical transmission of drive systems | 10 |
| 2.2.1 Rack and pinion | 11 |
| 2.2.2 Piezoelectric drive system | 11 |
| 2.2.3 Direct drive system | 12 |
| 2.2.4 Ball screw drive system | 14 |
| 2.3 Performance measure for machine tools | 15 |
| 2.3.1 Performance measure in time domain | 17 |
| 2.3.2 Performance measure in frequency domain | 18 |
| 2.4 Disturbance forces in machine tools application | 19 |
| 2.4.1 Mechanical resonance of the plant | 19 |
| 2.4.2 Mass variation | 20 |

| | | |
|-----------|---|-----------|
| 2.4.3 | Friction force | 21 |
| 2.4.4 | Cutting force | 23 |
| 2.5 | Cutting force measurement techniques | 26 |
| 2.5.1 | Capacitive displacement sensor | 26 |
| 2.5.2 | Current-sensor-based | 27 |
| 2.5.3 | Active electromagnetic bearings | 28 |
| 2.5.4 | Dynamometer | 29 |
| 2.6 | Controller design compensation techniques | 31 |
| 2.6.1 | Classical control technique | 31 |
| 2.6.1.1 | PID controller | 32 |
| 2.6.1.2 | Cascade controller | 36 |
| 2.6.2 | Advanced control techniques | 39 |
| 2.6.2.1 | Nonlinear PID (N-PID) and nonlinear cascade feed forward (NCasFF) | 40 |
| 2.6.2.2 | Sliding mode control (SMC) | 42 |
| 2.6.2.3 | H-infinity | 44 |
| 2.6.2.4 | Gain scheduling | 45 |
| 2.6.3 | State estimation control techniques | 47 |
| 2.6.3.1 | Disturbance observer | 48 |
| 2.6.3.2 | Kalman filter | 49 |
| 2.7 | Research gap | 51 |
| 3. | METHODOLOGY | 58 |
| 3.1 | Introduction | 58 |
| 3.2 | Design guidelines of a IMBDO plus DFO control structure | 61 |
| 3.3 | Experimental setup | 63 |
| 3.4 | System identification and system modelling | 65 |
| 3.5 | Identification of the motor constant | 71 |
| 3.6 | Cutting force measurement and characterization | 72 |
| 3.6.1 | Experimental setup of cutting force measurement | 73 |
| 3.6.2 | Characterization of the measured cutting force | 76 |
| 3.6.3 | Characterization and analysis of cutting forces | 79 |
| 3.6.4 | Analysis of the measured cutting forces | 79 |
| 3.7 | Summary | 81 |
| 4. | DESIGN OF CONTROLLERS AND STATE OBSERVER | 83 |
| 4.1 | Introduction | 83 |
| 4.2 | Design and analysis of cascade P/PI controller | 84 |
| 4.2.1 | Design and analyses of velocity control loop | 86 |
| 4.2.2 | Design and analyses of position control loop | 90 |
| 4.2.3 | Controller design validation | 95 |
| 4.3 | Design of inverse model-based disturbance observer | 97 |

| | | |
|-----------|---|------------|
| 4.3.1 | Design and stability analysis of Q -filter | 98 |
| 4.3.2 | Loops characteristic with inverse model-based disturbance observer | 102 |
| 4.3.3 | Inverse model-based disturbance observer design validation | 112 |
| 4.4 | Design structure of disturbance force observer | 113 |
| 4.4.1 | Analyses of disturbance force observer | 117 |
| 4.5 | Design structure of a state observer inverse model-based disturbance observer (IMBDO) with disturbance force observer (DFO) | 122 |
| 4.5.1 | Analysis loop of IMBDO plus DFO controller | 124 |
| 4.6 | Summary | 128 |
| 5. | RESULTS AND DISCUSSION | 130 |
| 5.1 | Introduction | 130 |
| 5.2 | Numerical performance analyses | 131 |
| 5.2.1 | Control performances of cascade P/PI | 131 |
| 5.2.1.1 | Maximum tracking error | 133 |
| 5.2.1.2 | RMSE of tracking errors | 135 |
| 5.2.1.3 | FFT of tracking error | 137 |
| 5.2.2 | Control performances of cascade P/PI with inverse model-based disturbance observer | 139 |
| 5.2.2.1 | Maximum tracking error | 141 |
| 5.2.2.2 | RMSE of tracking errors | 142 |
| 5.2.2.3 | FFT of tracking error | 144 |
| 5.2.3 | Control performances of cascade P/PI with disturbance force observer | 146 |
| 5.2.3.1 | Maximum tracking error | 148 |
| 5.2.3.2 | RMSE of tracking errors | 149 |
| 5.2.3.3 | FFT of tracking error | 150 |
| 5.2.4 | Control performances for cascade P/PI with both inverse model-based disturbance observer and disturbance force observer | 153 |
| 5.2.4.1 | Maximum tracking error | 157 |
| 5.2.4.2 | RMSE of tracking errors | 159 |
| 5.2.4.3 | FFT of tracking error | 160 |
| 5.3 | Experimental performance analyses | 162 |
| 5.3.1 | Control performances of cascade P/PI | 162 |
| 5.3.1.1 | Maximum tracking error | 163 |
| 5.3.1.2 | RMSE of tracking errors | 165 |
| 5.3.1.3 | FFT of tracking error | 166 |

| | | |
|-----------|---|------------|
| 5.3.2 | Control performances of cascade P/PI with inverse model-based disturbance observer | 168 |
| 5.3.2.1 | Maximum tracking error | 169 |
| 5.3.2.2 | RMSE of tracking errors | 171 |
| 5.3.2.3 | FFT of tracking error | 172 |
| 5.3.3 | Control performances of cascade P/PI with disturbance force observer | 174 |
| 5.3.3.1 | Maximum tracking error | 176 |
| 5.3.3.2 | RMSE of tracking errors | 178 |
| 5.3.3.3 | FFT of tracking error | 179 |
| 5.3.4 | Control performances for cascade P/PI with both inverse model-based disturbance observer and disturbance force observer | 182 |
| 5.3.4.1 | Maximum tracking error | 184 |
| 5.3.4.2 | RMSE of tracking errors | 186 |
| 5.3.4.3 | FFT of tracking error | 188 |
| 5.4 | Discussion on control performances | 190 |
| 5.4.1 | Analysis of maximum tracking errors | 190 |
| 5.4.2 | Analysis of RMSE tracking errors | 194 |
| 5.4.3 | Analysis of FFT of tracking errors | 197 |
| 5.4.4 | Analysis of closed loop characteristics and sensitivity function | 201 |
| 5.5 | Summary of results | 205 |
| 6. | CONCLUSIONS AND FUTURE RECOMMENDATIONS | 211 |
| 6.1 | Overview | 211 |
| 6.2 | Significant findings | 212 |
| 6.3 | Future recommendation | 215 |
| | REFERENCES | 217 |
| | APPENDICES | 239 |

LIST OF TABLES

| TABLE | TITLE | PAGE |
|-------|--|------|
| 2.1 | Effects of each controller parameter k_p , k_i and k_d on a closed loop system | 33 |
| 2.2 | Summary of literature reviews on classical control techniques | 53 |
| 2.3 | Summary of literature reviews on advanced control techniques | 54 |
| 2.4 | Summary of literature reviews on state estimation control-based techniques | 55 |
| 3.1 | Parameters of system model | 68 |
| 3.2 | List of equipment with specifications | 73 |
| 3.3 | Recommended cutting parameters for milling operation | 77 |
| 3.4 | Cutting parameters of the experimental design | 77 |
| 3.5 | Amplitude cutting force at different spindle speed | 81 |
| 4.1 | Gain values of k_p and k_i for PI controller in velocity-loop | 87 |
| 4.2 | Gain margin and phase margin of the velocity open loop | 87 |
| 4.3 | Gain margin and phase margin of the position open loop | 91 |
| 4.4 | Bandwidths of velocity and position control loops | 95 |
| 4.5 | Characteristics of Q -filter | 102 |
| 4.6 | Gain margin and phase margin of velocity open loop transfer function | 104 |
| 4.7 | Gain margin and phase margin of the position open loop | 109 |
| 4.8 | Bandwidth of the position loops | 110 |

| | | |
|------|---|-----|
| 5.1 | Research configurations | 131 |
| 5.2 | Summary of input reference signal and input disturbance signal characteristics | 132 |
| 5.3 | Summary of MTE values for disturbance-free and disturbance-induced of one, two, and three harmonic frequency contents | 134 |
| 5.4 | Summary of RMSE values for disturbance-free and disturbance-induced of one, two, and three harmonic frequency contents | 136 |
| 5.5 | FFT of tracking error magnitudes for disturbance-free and disturbance-induced of one, two, and three harmonic frequency contents | 138 |
| 5.6 | Summary of input reference signal and input disturbance signal characteristics | 139 |
| 5.7 | Summary of MTE values for sinusoidal input disturbance of one, two and three frequency harmonics using cascade P/PI controller and a cascade P/PI embedded with IMBDO | 142 |
| 5.8 | Summary of RMSE values for one, two and three harmonic frequency contents for cascade P/PI controller and a cascade P/PI embedded with IMBDO | 144 |
| 5.9 | Summary of FFT peak magnitude values of tracking error for cases with and without disturbance observer | 145 |
| 5.10 | Summary of input reference signal and input disturbance signal characteristics | 146 |
| 5.11 | Summary of MTE values for sinusoidal input disturbance of one, two and three frequency harmonics using cascade P/PI controller and a cascade P/PI embedded with DFO | 149 |
| 5.12 | Summary of RMSE values for one, two and three harmonic frequency contents for cascade P/PI controller and a cascade P/PI embedded with DFO | 150 |

| | | |
|------|--|-----|
| 5.13 | Summary of FFT peak magnitude values of tracking error for cases with and without disturbance observer | 152 |
| 5.14 | Summary of input reference signal and input disturbance signal characteristics | 156 |
| 5.15 | Summary of MTE values for sinusoidal input disturbance of one, two and three frequency harmonics using cascade P/PI controller and a cascade P/PI embedded with IMBDO plus DFO | 158 |
| 5.16 | Summary of RMSE values for one, two and three harmonic frequency contents for cascade P/PI controller and a cascade P/PI embedded with IMBDO plus DFO | 160 |
| 5.17 | Summary of FFT peak magnitude values of tracking error for cases with and without disturbance observer | 161 |
| 5.18 | Summary of input reference signal and input disturbance signal characteristics | 162 |
| 5.19 | Summary of MTE values for disturbance-free and disturbance-induced of one, two, and three harmonic frequency contents | 164 |
| 5.20 | Summary of RMSE values for disturbance-free and disturbance-induced of one, two, and three harmonic frequency contents | 166 |
| 5.21 | Summary of FFT peak magnitude values of tracking error for cases with and without input disturbance signal | 167 |
| 5.22 | Summary of input reference signal and input disturbance signals characteristics | 168 |
| 5.23 | Summary of MTE values for input disturbance of one, two and three harmonics for a cascade P/PI controller and a cascade P/PI with IMBDO | 170 |
| 5.24 | Summary of RMSE values input sinusoidal signal of one, two and three harmonics for a cascade P/PI controller and cascade P/PI embedded with IMBDO | 172 |

| | | |
|------|--|-----|
| 5.25 | Summary of FFT peak magnitude values of tracking error for cases with and without disturbance observer | 174 |
| 5.26 | Summary of input reference signal and input disturbance signal characteristics | 175 |
| 5.27 | Summary of MTE values for input disturbance of one, two and three harmonics for a cascade P/PI and a cascade P/PI with DFO | 178 |
| 5.28 | Summary of RMSE values input sinusoidal signal of one, two and three harmonics for a cascade P/PI controller and cascade P/PI embedded with DFO | 179 |
| 5.29 | Summary of FFT peak magnitude values of tracking error for cases with and without disturbance observer | 182 |
| 5.30 | Summary of input reference signal and input disturbance signal characteristics | 183 |
| 5.31 | Summary of MTE values for input disturbance of one, two and three harmonics for a cascade P/PI and a cascade P/PI with IMBDO plus DFO | 186 |
| 5.32 | Summary of RMSE values input sinusoidal signal of one, two and three harmonics for a cascade P/PI controller and cascade P/PI embedded with IMBDO plus DFO | 187 |
| 5.33 | Summary of FFT peak magnitude values of tracking error for cases with and without disturbance observer | 189 |
| 5.34 | Comparison between numerical and experimental values of maximum tracking error for four different control configurations at different harmonic frequency contents | 191 |
| 5.35 | Comparison between numerical and experimental values of percentage error reduction relating to maximum tracking error for four different control configurations at different harmonic frequency contents | 192 |

| | | |
|------|--|-----|
| 5.36 | Comparison in numerical and experimental values of RMSE of four different control configurations and harmonic frequency contents | 195 |
| 5.37 | Comparison in numerical and experimental values of percentage error reduction in RMSE for four different control configurations and harmonic frequency contents | 195 |
| 5.38 | Comparison between numerical and experimental values of FFT tracking error for four different control configurations and harmonic frequency contents | 200 |
| 5.39 | Comparison between numerical and experimental values of percentage error reduction of FFT magnitudes for four different control configurations and harmonic frequency contents | 200 |
| 5.40 | Summary of control performance measures of single input harmonic for different control configurations | 210 |
| 5.41 | Summary of control performances measures of double input harmonics for different control configurations | 210 |
| 5.42 | Summary of control performances measures of triple input harmonics for different control configurations | 210 |

LIST OF FIGURES

| FIGURE | TITLE | PAGE |
|--------|---|------|
| 2.1 | Rack and pinion drive system | 11 |
| 2.2 | General structure of a piezoelectric drive system | 12 |
| 2.3 | (a) Direct drive system and (b) Structure of iron-core linear drive system | 13 |
| 2.4 | Ball screw drive system | 15 |
| 2.5 | Point-to-point motion control | 16 |
| 2.6 | Continuous motion control | 16 |
| 2.7 | Transient response specifications of a second order system | 18 |
| 2.8 | FRF measurement for different machine conditions (bolted and unbolted) | 20 |
| 2.9 | Different combinations of linear motor modules | 21 |
| 2.10 | Quadrant glitches in circular test | 22 |
| 2.11 | Cutting parameter direction in the cutting zone | 23 |
| 2.12 | Original cutting force data from milling operation | 25 |
| 2.13 | A spindle integrated with displacement sensor system | 27 |
| 2.14 | Schematic illustrations of current-sensor-based cutting force sensing technique | 28 |
| 2.15 | Structure of active electromagnetic bearings | 29 |
| 2.16 | Kistler force measurement dynamometer | 30 |
| 2.17 | General structure of control system with a PID controller | 32 |

| | | |
|------|---|----|
| 2.18 | Block diagram of a basic PID controller with external disturbance and feedback control system | 34 |
| 2.19 | Structure of cascade P/PI controller | 37 |
| 2.20 | Block diagram of N-PID controller in feedback system | 40 |
| 2.21 | Chattering phenomenon | 43 |
| 2.22 | The general control configuration to synthesize controller using H-infinity | 44 |
| 2.23 | Block diagram of gain scheduling controller | 46 |
| 2.24 | General block diagram of state estimation techniques | 47 |
| 2.25 | Summary of literature review | 57 |
| 3.1 | Overall flow chart of the research methodology | 60 |
| 3.2 | Flowchart of design guidelines of combine IMBDO plus DFO | 62 |
| 3.3 | (a) XY positioning milling table ball screw driven system by Googol Tech Series (b) Schematic diagram of the XY positioning milling table | 63 |
| 3.4 | Configuration of overall experimental setup | 65 |
| 3.5 | Open-loop Simulink diagram of FRF measurement for XY positioning milling table ball screw driven system | 66 |
| 3.6 | Measured open loop FRF of x -axis positioning system | 67 |
| 3.7 | Measured FRF and fitted second order model with time delay | 68 |
| 3.8 | Time delay from Bode plot for second order transfer function | 69 |
| 3.9 | A schematic of mass-spring-damper system | 70 |
| 3.10 | Block diagram of the open loop system for motor constant identification and force estimation | 71 |
| 3.11 | Schematic diagram for cutting force characterization | 74 |
| 3.12 | Mounting points of the Kistler Dynamometer | 75 |

| | | |
|------|--|----|
| 3.13 | Aluminium block during milling operation | 76 |
| 3.14 | An overview of cutting force during milling process | 76 |
| 3.15 | Cutting path planning for cutting force measurement | 78 |
| 3.16 | An example of measured cutting force signal at 1500 rpm spindle speed | 78 |
| 3.17 | An example of insertion of measured cutting forces into the control system | 79 |
| 3.18 | FFT of cutting forces at (a) 1500 rpm, (b) 2500 rpm and (c) 3000 rpm spindle speed rotation | 80 |
| 4.1 | General scheme of a cascade P/PI control structure | 85 |
| 4.2 | Block diagram of velocity control loop | 86 |
| 4.3 | Bode diagram of velocity open loop transfer function with gain margin of 9.37 dB at 194 Hz and phase margin of 56.4° at 96.4 Hz | 88 |
| 4.4 | Nyquist plot of the velocity open loop transfer function | 88 |
| 4.5 | Bode diagram of velocity closed-loop transfer function | 89 |
| 4.6 | Sensitivity function of the velocity loop | 89 |
| 4.7 | Bode diagram of position open loop transfer function with a gain margin of 9.1 dB at 123 Hz and a phase margin of 67.1° at 31.4 Hz | 92 |
| 4.8 | Nyquist plot of position control loop | 92 |
| 4.9 | Bode diagram of position closed-loop transfer function | 93 |
| 4.10 | Sensitivity function of position control loop | 93 |
| 4.11 | Peak value of magnitude plot for sensitivity function of the position | 94 |
| 4.12 | Loop peak value of magnitude plot for position closed-loop transfer function | 95 |

| | | |
|------|---|-----|
| 4.13 | (a) Position error transfer function and, (b) simulated tracking error of the x -axis for sinusoidal reference signal of an amplitude of 10 mm and frequency 0.5 Hz | 96 |
| 4.14 | Block diagram of a system with an inverse model-based disturbance observer and Q -filter | 97 |
| 4.15 | Equivalent block diagram of a system with an inverse model-based disturbance observer and Q -filter | 98 |
| 4.16 | Magnitude plot and bandwidth limitation of the Q -filter | 101 |
| 4.17 | Schematic diagram of the cascade P/PI position control with an inverse model-based disturbance observer | 102 |
| 4.18 | Cascade P/PI position control with equivalent block diagram of the inverse model-based disturbance observer | 103 |
| 4.19 | Bode diagram of velocity open loop transfer function for system with and without disturbance observer | 104 |
| 4.20 | Velocity closed loop transfer functions for x -axis for system with and without a disturbance observer | 105 |
| 4.21 | Effect of the disturbance observer on the velocity loop sensitivity transfer functions for x -axis | 106 |
| 4.22 | Nyquist plots of the velocity loops with and without the disturbance observer | 106 |
| 4.23 | Position open loop transfer function for the system with and without a disturbance observer | 108 |
| 4.24 | Position closed-loop transfer functions of for system with and without a disturbance observer | 109 |
| 4.25 | Comparison in sensitivity function of the position loop | 110 |
| 4.26 | Effect of the disturbance observer on the sensitivity function of; (a) velocity and (b) position open loop | 111 |

| | | |
|------|--|-----|
| 4.27 | Nyquist plots of the position loops with and without the disturbance observer | 111 |
| 4.28 | (a) Simulated tracking error and, (b) position error transfer functions for sinusoidal reference signal of amplitude 10 mm and frequency 0.5 Hz | 113 |
| 4.29 | Schematic diagram of cascade P/PI position controller with DFO | 115 |
| 4.30 | Schematic diagram of a force observer structure (single harmonic) | 116 |
| 4.31 | Sensitivity function for one harmonic, two harmonics and three harmonics | 121 |
| 4.32 | Bode diagram of closed loop transfer function of the system with DFO designed for one harmonic, two harmonics and three harmonics frequencies | 121 |
| 4.33 | The effect of a disturbance observer on tracking errors for disturbance input frequencies of one harmonic, two harmonics and three harmonics | 122 |
| 4.34 | Control structure of cascade P/PI with combined inverse model-based disturbance observer plus disturbance force observer for single harmonic frequency | 123 |
| 4.35 | Bode plots of sensitivity function for single harmonic with add-on module state-observer based controller | 126 |
| 4.36 | Bode plots of sensitivity function for double harmonic with add-on module state-observer based controller | 126 |
| 4.37 | Bode plots of sensitivity function for triple harmonic with add-on module state-observer based controller | 127 |
| 4.38 | Bode diagram of closed loop of the system DFO plus IMBDO with one harmonic, two harmonics and three harmonics | 127 |
| 4.39 | The effect of state observer-based IMBDO plus DFO is activated | 128 |
| 5.1 | Schematic diagram for numerical analysis of cascade P/PI controller | 132 |

| | | |
|------|---|-----|
| 5.2 | Numerical values of MTE for cases without input disturbance and with input disturbance of (a) one harmonic, (b) two harmonics, and (c) three harmonics | 133 |
| 5.3 | Numerical values of RMSE for cases without input disturbance and with input disturbance of (a) one harmonic, (b) two harmonics, and (c) three harmonics | 136 |
| 5.4 | FFT spectral analysis of the position tracking errors without input disturbance (in the middle) and with input disturbance (in the bottom) for (a) one, (b) two and (c) three harmonic contents | 138 |
| 5.5 | MATLAB/Simulink diagram of a cascade P/PI controller and a disturbance observer with a sinusoidal based disturbance input signal | 140 |
| 5.6 | The effect of a disturbance observer on tracking errors for disturbance input frequencies of (a) 0.2 Hz, (b) 0.2 Hz and 0.5 Hz, and (c) 0.2 Hz, 0.5 Hz and 0.8 Hz | 140 |
| 5.7 | Numerical values of MTE for input disturbance of (a) one harmonic, (b) two harmonics, and (c) three harmonics for cases with and without observers | 141 |
| 5.8 | Numerical values of RMSE for sinusoidal input disturbance of (a) one harmonic, (b) two harmonics, and (c) three harmonics with and without disturbance observer | 143 |
| 5.9 | FFT results of position errors without the disturbance observer (in the middle) and with the disturbance observer (in the bottom) for one, two and three harmonic contents | 145 |
| 5.10 | Schematic diagram of the control structure that includes the cascade P/PI position controller without observer feedback | 146 |
| 5.11 | Schematic diagram of a cascade P/PI controller with observer feedback | 147 |

| | | |
|------|---|-----|
| 5.12 | Effect of disturbance observer on tracking errors for disturbance input frequencies of (a) 0.2 Hz, (b) 0.2 Hz and 0.5 Hz, and (c) 0.2 Hz, 0.5 Hz and 0.8 Hz with input reference signal of 0.5 mm amplitude and frequency of 1 Hz | 147 |
| 5.13 | Numerical values of MTE for input disturbance of (a) one harmonic, (b) two harmonics, and (c) three harmonics for cases with and without observers | 148 |
| 5.14 | Numerical values of RMSE for sinusoidal input disturbance of (a) one harmonic, (b) two harmonics, and (c) three harmonics with and without disturbance observer | 150 |
| 5.15 | FFT results indicating initial spikes | 151 |
| 5.16 | FFT results of position errors without the disturbance observer (in the middle) and with the disturbance observer (in the bottom) for one, two and three harmonic contents | 152 |
| 5.17 | Schematic diagrams of the control structure including cascade P/PI position controller with both IMBDO (purple line) and DFO (green line) without observer feedback | 154 |
| 5.18 | Schematic diagram of the control structure including cascade P/PI position controller with both IMBDO (purple line) and DFO (green line) with observer feedback | 154 |
| 5.19 | Effect of IMBDO plus DFO on tracking errors for input disturbance frequencies of (a) single harmonic (0.2 Hz), (b) double harmonics (0.2 Hz and 0.5 Hz), and (c) triple harmonics (0.2 Hz, 0.5 Hz and 0.8 Hz) | 155 |
| 5.20 | Spectral analysis of position error for disturbance observer with unmatched harmonics | 156 |
| 5.21 | Numerical values of MTE for input disturbance of (a) one harmonic, (b) two harmonics, and (c) three harmonics for cases with and without observers | 158 |